Eur. Phys. J. C 38, 483–494 (2005)
Digital Object Identifier (DOI) 10.1140/epjc/s2004-02062-5

THE EUROPEAN PHYSICAL JOURNAL C

# Quark–meson $SU(3)$ model in a Tamm–Dancoff inspired approximation

D. Horvat[1,a,b], D. Horvatić[2,c], D. Tadić[2]

[1] Physics Department, Faculty of Electrical Engineering, University of Zagreb, Unska 3, 10000 Zagreb, Croatia
[2] Physics Department, University of Zagreb, Bijenička c. 32, 10000 Zagreb, Croatia

Received: 24 August 2004 /
Published online: 1 December 2004 – 

**Abstract.** The non-linear chiral quark–meson $U(3)\times U(3)$ model is solved using the Tamm–Dancoff inspired approximation which is described in an earlier paper [Phys. Rev. D 58, 034003 (1998)]. The resulting system of 15 coupled non-linear differential equations self-consistently determines all quark–meson coupling constants. Also the obtained solutions for quark and meson fields are stable and physically acceptable. As the zeroth approximation of a more refined structure they were used to calculate $SU(3)$ baryon octet magnetic moments and axial coupling constants with baryon state vectors containing valence quarks only, at this primordial level. The results are very promising, so possibilities to pursuit more sophistication and improved physical input is indicated.

**PACS.** 12.39.Ba, 12.39.Fe

## 1 Introduction

The Tamm–Dancoff inspired approximation (TDIA) [1] was applied some time ago to the chiral quark–meson model based on the $SU(2)$ linear $\sigma$ model [2,3]. The results are comparable to those obtained using the hedgehog Ansätze [4–7]. That is to some extent understandable as both methods lead to similarly looking sets of equations for meson solitons (fields). All details of the TDIA are described in [1]. It is well known that the Tamm–Dancoff method [8] is a better approximation than the perturbation theory, so it is a natural environment within which one dares to attack more ambitious problems, with many more degrees of freedom.

In [1] the two-flavor linear $\sigma$ model was used as a transparent example for the application of TDIA. Recently the three-flavor meson $U(3)\times U(3)$ octets were investigated [9–11] and it has been stated [10,11] that the linear $\sigma$ model with three flavors works much better than what was generally believed. As regards the differences with the non-linear version, in the linear $\sigma$ model one can treat both scalar and pseudoscalar nonets simultaneously. The scalars are the chiral partners of $\pi$, $\eta$, etc. and the analysis strongly suggests that they, like the pseudoscalars, are $\bar{q}q$ states [10,11]. Such theoretical conclusions made the TDIA approach quite attractive as in that approximation mesons (solitons) naturally appear, in the lowest order as $\bar{q}q$ states. In TDIA one works in the Heisenberg picture [12], expands field operators in the free field creation and annihilation operators and then truncates the expansion usually at the $t=0$ level ($t$ being the usual Mandelstam variable). That leads automatically, after truncations at the $q^2=0$ level, to meson fields (soliton phases) which depend on bilinear combinations of quark/antiquark operators only, i.e. to $\bar{q}q$ structures. (The richer meson–quark structure is discussed in the last section concerning extensions and refinement of this basic model.)

The chiral quark/meson $U(3)\times U(3)$ model under consideration has the familiar form which was used previously when the $SU(2)$ model [5,6] was enlarged by cranking involving intrinsic flavor space [7]. The system of non-linear differential equations obtained here bears some similarity to the systems obtained by using hedgehog Ansätze [5–7]. It has been argued that the linear $\sigma$ model [10,11] and its close relative the quark–meson model [7] might capture the essential features of QCD in the low energy region, while being easier to handle than the complex exact quark–gluon theory. The TDIA treatment of the $U(3)\times U(3)$ quark–gluon model thus might give some physical insights in the baryon structure.

The lowest order TDIA leads to the coupled system of 15 non-linear differential equations and 21 boundary conditions for meson octet pseudoscalar and scalar profile functions. That problem is completely solvable, as will be outlined below. The strengths of the quark–meson couplings are self-consistently determined by the system. Although the chiral bag formalism for quarks and mesons

[a] *Correspondence to:* davorh@phy.hr
[b] e-mail: dubravko.horvat@fer.hr
[c] e-mail: davorh@phy.hr

is used here [1,13] the spherical cavity approximation for quarks in principle can be dropped. That would lead to a larger system of equations but it would also mean that $q^2 \neq 0$ level is reached. At this level more sophisticated renormalization-group dependent coupling constants and baryon wave functions would be required. This kind of improvements are envisaged as a further refinement of the model.

The structure of this model [1] presented in the next two sections is very transparent and all of its features are always discernible. One can see directly how the approximate baryon states, made of valence quarks only [14,15], perform. In order to do that one calculates the matrix elements of the (approximate) Heisenberg operators. Matrix elements at the $q^2 = 0$ level are evaluated using meson profile fuctions obtained by the numerical procedure explained in Sect. 4. As in TDIA the isospin (and hypercharge) and spin are separably conserved, the solutions are used to calculate magnetic moments and axial-vector coupling constants for the baryon octet in Sects. 5 and 6. The results discussed in Sect. 7 indicate the need for richer structure ($s\bar{s}$ pairs etc.) of baryon state vectors [16] and for the inclusion of exchange current corrections [17].

## 2 Model formalism

TDIA has been already described in some detail elsewhere [1]. Here we give some particulars concerning the quark linear $\sigma$ model and TDIA approximation. The Lagrangian in which the linear $\sigma$ model is embedded in the bag environment has the well known form [1,6,19]

$$\mathcal{L} = \mathcal{L}_\psi \Theta + \mathcal{L}_{\rm int}\delta_S + [\mathcal{L}_\chi + U(\chi)]\overline{\Theta}\,. \tag{2.1}$$

Here all pieces, except for the symmetry breaking $\mathcal{L}_{\rm SB}$ one, are $U(3)\times U(3)$ invariant [3,7,11] i.e.

$$\begin{aligned}
\mathcal{L}_\psi &= \frac{\mathrm{i}}{2}\left(\overline{\psi}\gamma^\mu\partial_\mu\psi - \partial_\mu\overline{\psi}\gamma^\mu\psi\right),\\
\mathcal{L}_{\rm int} &= \frac{g}{2}\overline{\psi}\left(\sigma_a + \mathrm{i}\pi_a\gamma_5\right)\lambda^a\psi\,,\\
\mathcal{L}_\chi &= \frac{1}{2}\left(\partial^\mu\sigma_a\partial_\mu\sigma_a + \partial^\mu\pi_a\partial_\mu\pi_a\right),\\
U(\chi) &= -\frac{1}{2}\mu^2\left(\sigma_a^2+\pi_a^2\right) - \frac{1}{4}\lambda^2\left(\sigma_a^2+\pi_a^2\right)^2 + \mathcal{L}_{\rm SB}\,.
\end{aligned} \tag{2.2}$$

Here ($\sigma^a$, $\pi^a$, $a = 0,1,\ldots,8$) are (scalar, pseudoscalar) $U(3)$ nonets [9–11]. The symmetry is broken in a minimal way by the vacuum expectation values of the $U(3)$ scalars $\sigma$ and $\zeta$ [11]

$$\begin{aligned}
\mathcal{L}_{\rm SB} &= m_\pi^2 f_\pi\sigma + \frac{(2m_K^2 f_K - m_\pi^2 f_\pi)}{\sqrt{2}}\zeta\,,\\
\sigma_{\rm vac} &= f_\pi \Rightarrow \sigma \to \sigma - f_\pi\,,\\
\zeta_{\rm vac} &= \frac{(2f_K - f_\pi)}{\sqrt{2}} \Rightarrow \zeta \to \zeta - \zeta_{\rm vac}\,.
\end{aligned} \tag{2.3}$$

That leaves pseudoscalar (scalar) masses in the corresponding $U(3)$ nonets degenerate at this level of approximation. Multiplet splitting is however partly implemented by assigning different quark–meson coupling constants in $\mathcal{L}_{\rm int}$ (see Sect. 3 below). The pseudoscalar $\pi_a$ and scalar $\sigma_a$ nonets enter in the interaction $U(\chi)$ term (2.3) as follows:

$$\begin{aligned}
\sigma_a^2 &= a_0^+a_0^- + a_0^-a_0^+ + {a_0^0}^2 + \kappa^+\kappa^- + \kappa^-\kappa^+\\
&\quad + \overline{\kappa^0}\kappa^0 + \kappa^0\overline{\kappa^0} + \sigma^2 + \zeta^2\,,\\
\pi_a^2 &= \pi^+\pi^- + \pi^-\pi^+ + {\pi^0}^2 + K^+K^- + K^-K^+\\
&\quad + \overline{K^0}K^0 + K^0\overline{K^0} + \eta^2 + {\eta'}^2\,.
\end{aligned} \tag{2.4}$$

The interaction with the quark field $\bar{\psi} = (\bar{u},\bar{d},\bar{s})$ is determined by the standard $U(3)$ $\lambda_i$ matrices:

$$\begin{aligned}
\sigma_a\lambda^a &= a_0^+\lambda_{12}^- + a_0^-\lambda_{12}^+ + a_0^0\lambda_3 + \kappa^+\lambda_{45}^- + \kappa^-\lambda_{45}^+\\
&\quad + \overline{\kappa^0}\lambda_{67}^- + \kappa^0\lambda_{67}^+ + \sigma\lambda_{08}^- + \zeta\lambda_{08}^+\,,\\
\pi_a\lambda^a &= \pi^+\lambda_{12}^- + \pi^-\lambda_{12}^+ + \pi^0\lambda_3 + K^+\lambda_{45}^- + K^-\lambda_{45}^+\\
&\quad + \overline{K^0}\lambda_{67}^- + K^0\lambda_{67}^+ + \eta\lambda_{08}^+ + \eta'\lambda_{08}^-\,,\\
a &= 0,1,2,\ldots,8\,.
\end{aligned} \tag{2.5a}$$

$$\begin{aligned}
\lambda_{08}^+ &= \sqrt{\frac{1}{3}}\left(\sqrt{2}\lambda_0 + \lambda_8\right),\\
\lambda_{08}^- &= \sqrt{\frac{1}{3}}\left(\lambda_0 - \sqrt{2}\lambda_8\right), \qquad \lambda_0 = \sqrt{\frac{2}{3}}\mathbf{I}\,,\\
\lambda_{ij}^\pm &= \sqrt{\frac{1}{2}}\left(\lambda_i \pm \mathrm{i}\lambda_j\right) \quad (i,j = 1,2,\ldots,7).
\end{aligned} \tag{2.5b}$$

The standard variational procedure leads to the coupled system which contains 20 equations of motion, eight linear boundary conditions and 18 derivative boundary conditions involving quantum fields. However as the system retains a lot of symmetry in TDIA this gets reduced to a smaller set of c-equations. The above mentioned set of equations (i.e. q-equations) is listed in Appendix A. Here we sketch the TDIA procedure and list the non-linear system of c-equations which will be solved numerically.

The field operators $\psi$, $\sigma_a$ and $\pi_a$ appearing in (2.2) and in Appendix A are expanded in terms of the free field operators retaining only lowest (i.e. leading non-trivial contributions). What follows is the $U(3)\times U(3)$ generalization of the Ansätze used in [1]. The "driving" Ansätze are the ones for the quark fields. For the massless $u$ and $d$ fields one uses

$$\begin{aligned}
\psi_f^c &= \frac{N_0}{\sqrt{4\pi}}\left[\begin{pmatrix} f_0 \\ \mathrm{i}\,(\sigma\hat{r})\,g_0\end{pmatrix}\chi_\mu^f b_{\mu,f}^c\right.\\
&\quad \left. + \begin{pmatrix} (\sigma\hat{r})\,g_0 \\ \mathrm{i}f_0\end{pmatrix}\chi_\mu^{f\dagger} d_{\mu,\bar{f}}^{c\dagger}\right],\\
f_0 &= j_0\left(\frac{\omega_0 r}{R}\right), \quad g_0 = j_1\left(\frac{\omega_0 r}{R}\right),
\end{aligned} \tag{2.6}$$

$$N_0^2(\omega_0) = \frac{1}{R^3}\left[j_0^2(\omega_0) + j_1^2(\omega_0) - \frac{2j_0(\omega_0)j_1(\omega_0)}{\omega_0}\right]^{-1}.$$

The $SU(3)$ flavor symmetry is explicitly broken by assuming that the $s$-quark has a mass $m_s \neq 0$, with the corresponding Ansatz

$$\begin{aligned}
\psi_f^c &= \frac{N_m}{\sqrt{4\pi}} \left[ \begin{pmatrix} f_m \\ \mathrm{i}\,(\sigma\hat{r})\, g_m \end{pmatrix} \chi_\mu^f b_{\mu,f}^c \right. \\
&\quad \left. + \begin{pmatrix} (\sigma\hat{r})\, g_m \\ \mathrm{i} f_m \end{pmatrix} \chi_\mu^{f\dagger} d_{\mu,\bar{f}}^{c\dagger} \right] \\
f_m &= \sqrt{\frac{E+m_s}{E}}\, j_0\left(\frac{\omega_m r}{R}\right), \\
g_m &= \sqrt{\frac{E-m_s}{E}}\, j_1\left(\frac{\omega_m r}{R}\right), \\
E(m,R) &= \frac{1}{R}\sqrt{\omega^2 + (m_s R)^2}\,, \\
N_m^2(\omega_m) &= \frac{N_0^2(\omega_m)}{1 + N_0^2(\omega_m) N_R}\,, \\
N_R &= \frac{m_s j_0(\omega_m) j_1(\omega_m) R^3}{E\omega_m}\,. \qquad (2.7)
\end{aligned}$$

Here the indices $c$, $f$ and $\mu$ denote color, flavor and spin respectively.

The incorporation of $m \neq 0$ in the model structure is discussed in Appendix B. Boundary conditions involving quark fields [see (A22)–(A38)] determine (by use of the Ansätze (2.6) and (2.7)), the Ansätze for the meson fields. This matching then automatically produces mesons "made out of quark pairs", as suggested in the $\sigma$ model analysis [9–11]. One needs for pseudoscalar fields, for example,

$$\begin{aligned}
\pi^+ &= \pi_s^+(r) \left( b_{m,d}^{c\,\dagger} d_{m',\bar{u}}^{c\,\dagger} + d_{m,\bar{d}}^{c} b_{m',u}^{c} \right) \chi_m^\dagger \mathbf{1} \chi_{m'} \qquad (2.8a) \\
&\quad + \pi_p^+(r) \left( b_{m,d}^{c\,\dagger} b_{m',u}^{c} - d_{m',\bar{u}}^{c\,\dagger} d_{m,\bar{d}}^{c} \right) \chi_m^\dagger\, (\sigma\hat{r})\, \chi_{m'}\,, \\
K^+ &= K_s^+(r) \left( b_{m,s}^{c\,\dagger}\; d_{m',\bar{u}}^{c\,\dagger} + d_{m,\bar{s}}^{c}\; b_{m',u}^{c} \right) \chi_m^\dagger \mathbf{1} \chi_{m'} \qquad (2.8b) \\
&\quad + K_p^+(r) \left( b_{m,s}^{c\,\dagger} b_{m',u}^{c} - d_{m',\bar{u}}^{c\,\dagger} d_{m,\bar{s}}^{c} \right) \chi_m^\dagger\, (\sigma\hat{r})\, \chi_{m'}\,, \\
\eta &= \eta_s(r) \frac{1}{\sqrt{2}} \left( \left( b_{m,u}^{c\,\dagger} d_{m',\bar{u}}^{c\,\dagger} + b_{m,d}^{c\,\dagger} d_{m',\bar{d}}^{c\,\dagger} \right) \right. \\
&\quad \left. + \left( d_{m,\bar{u}}^{c} b_{m',u}^{c} + d_{m,\bar{d}}^{c} b_{m',d}^{c} \right) \right) \chi_m^\dagger \mathbf{1} \chi_{m'} \\
&\quad + \eta_p(r) \frac{1}{\sqrt{2}} \left( \left( b_{m,u}^{c\,\dagger} b_{m',u}^{c} + b_{m,d}^{c\,\dagger} b_{m',d}^{c} \right) \right. \qquad (2.8c) \\
&\quad \left. - \left( d_{m',\bar{u}}^{c\,\dagger} d_{m,\bar{u}}^{c} + d_{m',\bar{d}}^{c\,\dagger} d_{m,\bar{d}}^{c} \right) \right) \chi_m^\dagger\, (\sigma\hat{r})\, \chi_{m'}\,, \\
\eta' &= \eta_s'(r) \left( b_{m,s}^{c\,\dagger} d_{m',\bar{s}}^{c\,\dagger} + d_{m,\bar{s}}^{c} b_{m',s}^{c} \right) \chi_m^\dagger \mathbf{1} \chi_{m'} \qquad (2.8d) \\
&\quad + \eta_p'(r) \left( b_{m,s}^{c\,\dagger} b_{m',s}^{c} - d_{m',\bar{s}}^{c\,\dagger} d_{m,\bar{s}}^{c} \right) \chi_m^\dagger\, (\sigma\hat{r})\, \chi_{m'}\,.
\end{aligned}$$

Both scalar ($\pi_s$, $K_s$, $\eta_s$) and pseudoscalar ($\pi_p\sigma\hat{r}$, $\eta_p\sigma\hat{r}$ etc.) components of the pseudoscalar mesons are induced by the boundary conditions. The scalar parts formally correspond to physical "mesons" while the pseudoscalar ones are connected with the solitons. The solitons contribute to the baryonic current matrix elements as shown in Sect. 5 below. All those are just $U(3) \times U(3)$ generalizations of our earlier $U(2)$ based results [1]. For scalar fields, scalar and pseudoscalar contributions are reversed. All these mixings are a consequence of the transformation properties of the bilinear combination of creation/annihilation operators [15, 18]. Everything is again driven by boundary conditions which require the following:

$$\begin{aligned}
a_0^+ &= a_{0\,s}^+(r) \left( b_{m,d}^{c\,\dagger} b_{m',u}^{c} + d_{m',\bar{u}}^{c\,\dagger} d_{m,\bar{d}}^{c} \right) \chi_m^\dagger \mathbf{1} \chi_{m'}, \qquad (2.9a) \\
a_0^- &= a_{0\,s}^-(r) \left( b_{m,u}^{c\,\dagger} b_{m',d}^{c} + d_{m',\bar{d}}^{c\,\dagger} d_{m,\bar{u}}^{c} \right) \chi_m^\dagger \mathbf{1} \chi_{m'}, \qquad (2.9b) \\
\kappa^+ &= \kappa_s^+(r) \left( b_{m,s}^{c\,\dagger} b_{m',u}^{c} + d_{m',\bar{u}}^{c\,\dagger} d_{m,\bar{s}}^{c} \right) \chi_m^\dagger \mathbf{1} \chi_{m'} \qquad (2.9c) \\
&\quad + \kappa_p^+(r) \left( b_{m,s}^{c\,\dagger} d_{m',\bar{u}}^{c\,\dagger} - d_{m,\bar{s}}^{c} b_{m',u}^{c} \right) \chi_m^\dagger\, (\sigma\hat{r})\, \chi_{m'}\,, \\
\bar{\kappa}^0 &= \bar{\kappa}_s^0(r) \left( b_{m,d}^{c\,\dagger} b_{m',s}^{c} + d_{m',\bar{s}}^{c\,\dagger} d_{m,\bar{d}}^{c} \right) \chi_m^\dagger \mathbf{1} \chi_{m'} \qquad (2.9d) \\
&\quad + \bar{\kappa}_p^0(r) \left( b_{m,d}^{c\,\dagger} d_{m',\bar{s}}^{c\,\dagger} - d_{m,\bar{d}}^{c} b_{m',s}^{c} \right) \chi_m^\dagger\, (\sigma\hat{r})\, \chi_{m'}\,, \\
\sigma &= \sigma_s(r) \frac{1}{\sqrt{2}} \left( \left( b_{m,u}^{c\,\dagger} b_{m',u}^{c} + b_{m,d}^{c\,\dagger} b_{m',d}^{c} \right) \right. \\
&\quad \left. + \left( d_{m',\bar{u}}^{c\,\dagger} d_{m,\bar{u}}^{c} + d_{m',\bar{d}}^{c\,\dagger} d_{m,\bar{d}}^{c} \right) \right) \chi_m^\dagger \mathbf{1} \chi_{m'}\,, \qquad (2.9e) \\
\zeta &= \zeta_s(r) \left( b_{m,s}^{c\,\dagger} b_{m',s}^{c} + d_{m',\bar{s}}^{c\,\dagger} d_{m,\bar{s}}^{c} \right) \chi_m^\dagger \mathbf{1} \chi_{m'}\,. \qquad (2.9f)
\end{aligned}$$

Therefore $s$ states (solitons) contribute to the baryonic matrix elements.

The system of q-equations, which are listed in Appendix A, is in TDIA transformed in a system of differential c-equations. The operator equalities are expressed through the Ansätze (2.6)–(2.9). They are then sandwiched between suitable states. An example can be found in [1], (2.16). In addition we show here the treatment of the non-linear $\pi\sigma\sigma$ term which appears for example in (A23). Our simple Ansätze give a non-vanishing contribution for only a few of the intermediate states $|s_i\rangle$. With

$$\begin{aligned}
\langle f| = \langle q|\,, \quad |i\rangle = |q\rangle\,, \\
\langle f|\pi^a\sigma^a\sigma^a|i\rangle\,,
\end{aligned}$$

one obtains

$$\begin{aligned}
&\langle f|\pi^a\sigma^a\sigma^a|i\rangle = \langle 0|b_{d,e}^{c'}\pi^a|s_1\rangle\langle s_1|\sigma^a|s_2\rangle\langle s_2|\sigma^a b_{b,e'}^{c'\,\dagger}|0\rangle \\
&= \langle 0|b_{d,e}^{c'}\pi^a|s_1\rangle\langle s_1|\sigma^a|s_2\rangle\langle s_2|\sigma_s^a(r)\chi_{m_1}^\dagger \mathbf{1}\chi_{m_2}\,, \\
&b_{m_1,f_1}^{c\,\dagger} b_{m_2,f_2}^{c} b_{b,e'}^{c'\,\dagger}|0\rangle = \sigma_s^a(r)\chi_{m_1}^\dagger \mathbf{1}\chi_b\delta_{f_2,e'}, \\
&\langle 0|b_{d,e}^{c'}\pi^a|s_1\rangle\langle s_1|\sigma^a|s_2\rangle\langle s_2|b_{m_1,f_1}^{c'\,\dagger}|0\rangle \\
&= \sigma_s^a(r)\chi_{m_1}^\dagger \mathbf{1}\chi_b\delta_{f_2,e'}\langle 0|b_{d,e}^{c'}\pi^a|s_1\rangle\langle s_1|\sigma_s^a(r)\chi_{m_3}^\dagger \mathbf{1}\chi_{m_4}\,, \\
&b_{m_3,f_3}^{c\,\dagger} b_{m_4,f_4}^{c} b_{m_1,f_1}^{c'\,\dagger}|0\rangle \\
&= \sigma_s^{a\,2}(r)\chi_{m_3}^\dagger \mathbf{1}\chi_{m_1}\chi_{m_1}^\dagger \mathbf{1}\chi_b\delta_{f_2,e'}\delta_{f_4,f_1}\,,
\end{aligned}$$

$$\langle 0|b^{c'}_{d,e}\pi^a_p(r)\chi^\dagger_{m_5}(\sigma\hat{r})\,\chi_{m_6}b^{c\,\dagger}_{m_5,f_5}b^c_{m_6,f_6}b^{c'\,\dagger}_{m_3,f_3}|0\rangle$$
$$= 3\cdot\pi^a_p(r)\sigma^{a\,2}_s(r)\chi^\dagger_d(\sigma\hat{r})\,\chi_{m_3}\chi^\dagger_{m_3}\mathbf{1}\chi_{m_1}\chi^\dagger_{m_1}\mathbf{1}\chi_b\,,$$
$$\delta_{f_2,e'}\delta_{f_4,f_1}\delta_{f_6,f_3}\delta_{e,f_5} \qquad (2.10)$$
$$= 3\cdot\pi^a_p(r)\sigma^{a\,2}_s(r)\chi^\dagger_d(\sigma\hat{r})\,\chi_b\delta_{f_2,e'}\delta_{f_4,f_1}\delta_{f_6,f_3}\delta_{e,f_5}\,.$$

One ends with the profile function $\pi_p(r)$ (2.8), $\sigma_s(r)$ (2.9e) and with some Pauli matrices and spinors. In this way all the creation (annihilation) operators from the Ansätze and Appendix A can be contracted and one ends with the system listed in the following section.

## 3 Leading order in TDIA

As outlined above, in TDIA the model at the lowest oreder (i.e. at $t = q^2 = 0$) leads to a system of coupled ordinary non-linear differential equations and boundary conditions. This non-linear system contains scalar ($\pi_s(r)$, $K_s(r)$, ..., $a_{0,s}(r)$, $\kappa_s(r)$, ...) and pseudoscalar ($\pi_p(r)$, $K_p(r)$, ..., $\kappa_p(r)$, ...) profile functions (2.8) and (2.9):

$$D_0\pi_s+\lambda^2\pi_s\phi_1(r)=0\,,\ D_1\pi_p+\lambda^2\pi_p\phi_2(r)=0\,, \qquad (3.1)$$
$$D_0K_s+\lambda^2K_s\phi_1(r)=0\,,\ D_1K_p+\lambda^2K_p\phi_2(r)=0\,, \qquad (3.2)$$
$$D_0\eta_s+\lambda^2\eta_s\phi_1(r)=0\,,\ D_1\eta_p+\lambda^2\eta_p\phi_2(r)=0\,, \qquad (3.3)$$
$$D_0\eta'_s+\lambda^2\eta'_s\phi_1(r)=0\,,\ D_1\eta'_p+\lambda^2\eta'_p\phi_3(r)=0\,, \qquad (3.4)$$
$$D_0a_{0/s}+\lambda^2a_{0/s}\phi_2(r)=0\,,\ D_0\kappa_s+\lambda^2\kappa_s\phi_2(r)=0\,, \qquad (3.5)$$
$$D_1\kappa_p+\lambda^2\kappa_p\phi_1(r)=0\,, \qquad (3.6)$$
$$D_0\sigma_s+\lambda^2(\sigma_s-f_\pi)\phi_2(r)$$
$$+\lambda^2\left(\frac{1}{2}f_\pi^2+\zeta^2_{\rm vac}-\mu^2\right)f_\pi=0\,,$$
$$D_0\zeta_s+\lambda^2\left(\zeta_s-\zeta_{\rm vac}\right)\phi_3(r)$$
$$+\lambda^2\left(f_\pi^2+\zeta^2_{\rm vac}-\mu^2\right)\zeta_{\rm vac}=0\,. \qquad (3.7)$$

Here $\phi_1(r)$, $\phi_2(r)$, $\phi_3(r)$, $D_0$ and $D_1$ are defined by

$$\phi_1(r)=6\cdot(3\pi_s^2+4K_s^2+\eta_s^2+\eta_s'^{\,2}+4\kappa_p^2)$$
$$+\mu^2+f_\pi^2+\zeta^2_{\rm vac}\,,$$
$$\phi_2(r)=\frac{3}{2}\pi_p^2+K_p^2+\frac{1}{2}\eta_p^2+\frac{3}{2}a_{0/s}^2+\kappa_s^2$$
$$+\frac{1}{2}(\sigma_s-f_\pi)^2+\zeta^2_{\rm vac}+\mu^2\,, \qquad (3.8)$$
$$\phi_3(r)=2K_p^2+\eta_p'^{\,2}+2\kappa_s^2+(\zeta_s-\zeta_{\rm vac})^2+\mu^2+f_\pi^2\,,$$
$$D_0=\frac{\mathrm{d}^2}{\mathrm{d}r^2}+\frac{2}{r}\frac{\mathrm{d}}{\mathrm{d}r}\,,$$
$$D_1=\frac{\mathrm{d}^2}{\mathrm{d}r^2}+\frac{2}{r}\frac{\mathrm{d}}{\mathrm{d}r}-\frac{2}{r^2}\,.$$

Some additional explanations concerning the functions $\phi_2(r)$ and $\phi_3(r)$ are given in the following section. Through derivative boundary conditions the equations are connected with the quark radial functions $f_i(r)$, $g_j(r)$, i.e.

$$\partial_r a_{0/s}(R)=g_{a_0}N_{0,0}\left[f_0^2-g_0^2\right]\big|_{r=R}\,,$$
$$\partial_r\kappa_s(R)=g_\kappa N_{0,m}\left[f_mf_0-g_mg_0\right]\big|_{r=R}\,,$$
$$\partial_r\kappa_p(R)=g_\kappa N_{0,m}\left[f_mg_0-g_mf_0\right]\big|_{r=R}\,,$$
$$\partial_r\sigma_s(R)=g_\sigma N_{0,0}\left[f_0^2-g_0^2\right]\big|_{r=R}\,,$$
$$\partial_r\zeta_s(R)=g_\zeta N_{m,m}\left[f_m^2-g_m^2\right]\big|_{r=R}\,,$$
$$\partial_r\pi_s(R)=-g_\pi N_{0,0}\left[f_0^2+g_0^2\right]\big|_{r=R}\,,$$
$$\partial_r\pi_p(R)=-g_\pi N_{0,0}2f_0g_0\big|_{r=R}\,,$$
$$\partial_r K_s(R)=-g_K N_{0,m}\left[f_mf_0+g_mg_0\right]\big|_{r=R}\,,$$
$$\partial_r K_p(R)=-g_K N_{0,m}\left[f_mg_0+g_mf_0\right]\big|_{r=R}\,,$$
$$\partial_r\eta_s(R)=-g_\eta N_{0,0}\left[f_0^2+g_0^2\right]\big|_{r=R}\,,$$
$$\partial_r\eta_p(R)=-g_\eta N_{0,0}2f_0g_0\big|_{r=R}\,,$$
$$\partial_r\eta'_s(R)=-g_{\eta'}N_{m,m}\left[f_m^2+g_m^2\right]\big|_{r=R}\,,$$
$$\partial_r\eta'_p(R)=-g_{\eta'}N_{m,m}2f_mg_m\big|_{r=R}\,. \qquad (3.9a)$$

Here we have used the abbreviation

$$N_{i,j}=\frac{N_iN_j}{2\cdot 4\pi}\,,\quad i,j=0\ \text{ or }\ m\,. \qquad (3.9b)$$

The additional quark–"meson" connections are due to the linear boundary condition (A2), i.e.

$$J_0\left(1-g_\pi\pi_pN_1-g_\eta\eta_pN_2-g_KK_pN_n\right) \qquad (3.10a)$$
$$+\left(g_{a_0}a_{0/s}N_1+g_\sigma\left(\sigma_sN_2-f_\pi\right)+g_\kappa\kappa_sN_p\right)=0\,,$$
$$\left(1+g_\pi\pi_pN_1+g_\eta\eta_pN_2+g_KK_pN_p\right) \qquad (3.10b)$$
$$+J_0\left(g_{a_0}a_{0/s}N_1+g_\sigma\left(\sigma_sN_2-f_\pi\right)+g_\kappa\kappa_sN_n\right)=0\,,$$
$$1+g_\kappa\kappa_pN_p \qquad (3.10c)$$
$$=J_0\left(g_\sigma f_\pi+g_\pi\pi_sN_1+g_\eta\eta_sN_2+g_KK_sN_n\right)\,,$$
$$J_0\left(1+g_\kappa\kappa_pN_n\right) \qquad (3.10d)$$
$$=\left(g_\sigma f_\pi-g_\pi\pi_sN_1-g_\eta\eta_sN_2-g_KK_sN_p\right)$$
$$J_m\left(g_\zeta\left(\zeta_s-\zeta_{\rm vac}\right)+g_\kappa2\kappa_sN_n^{-1}\right)$$
$$+\left(1+g_{\eta'}\eta'_p+2K_pN_p^{-1}\right)=0\,, \qquad (3.10e)$$
$$g_\zeta\left(\zeta_s-\zeta_{\rm vac}\right)+g_\kappa2\kappa_sN_p^{-1}$$
$$=J_m\left(g_{\eta'}\eta'_p+2K_pN_n^{-1}-1\right)\,, \qquad (3.10f)$$
$$1+g_\kappa2\kappa_pN_p^{-1} \qquad (3.10g)$$
$$=J_m\left(g_\zeta\zeta_{\rm vac}+g_{\eta'}\eta'_s+g_K2K_sN_n^{-1}\right)\,,$$
$$J_m\left(1+g_\kappa2\kappa_pN_n^{-1}\right)$$
$$=J_m\left(g_\zeta\zeta_{\rm vac}-g_{\eta'}\eta'_s-g_K2K_sN_p^{-1}\right)\,. \qquad (3.10h)$$

These are algebraic relations in which all the functions as for example $J_0$, $\pi_p(r)$, $K_s(r)$ are evaluated at $r \equiv R$. Here $J_0$, $J_m$, $N_n$, $N_p$, $N_1$, $N_2$ are the following combinations:

$$J_0 = \frac{g_0}{f_0}\,, \quad J_m = \frac{g_m}{f_m}, \tag{3.11a}$$

$$N_n = \sqrt{\frac{1+N_0^2 N_R}{1+m/E}}\,, \quad N_p = \sqrt{\frac{1+N_0^2 N_R}{1-m/E}}, \tag{3.11b}$$

$$N_1 = \left(\frac{1}{\sqrt{2}}+1\right), \quad N_2 = \frac{1}{\sqrt{2}}. \tag{3.11c}$$

## 4 The numerical procedure

The numerical procedure is analogous to the one used by [1]. It relies on the code COLSYS, the collocation system solver developed by Ascher, Christiansen and Russel [20]. However, one should keep in mind that here one deals with a much larger system, which contains many novel features, and which stretches COLSYS to its upper bounds.

The symmetry breaking parameters assume the following values:

$$\begin{aligned} m_\pi &= 140\,\mathrm{MeV}\,, \quad f_\pi = 92.6\,\mathrm{MeV}\,, \\ m_K &= 494\,\mathrm{MeV}\,, \quad f_K = 113\,\mathrm{MeV}\,, \\ m_s &= 125\,\mathrm{MeV}\,, \quad R = 5\,\mathrm{GeV}^{-1}. \end{aligned} \tag{4.1}$$

The parameters $\mu$ and $\lambda$ from $U(\chi)$ (2.2) were selected by the requirement that all the profile functions appearing in (3.1) vanish at infinity. In TDIA all differential equations listed in Appendix A, but (A17) and (A19) fulfill that requirement. In TDIA (A17) and (A19) have the form

$$D_0\sigma_s + \lambda^2(\sigma_s - f_\pi)\phi_2(r) + m_\pi^2 f_\pi = 0 \tag{4.2}$$

$$D_0\zeta_s + \lambda^2\left(\zeta_s - \zeta_{\mathrm{vac}}\right)\phi_3(r) + \frac{\left(2m_K^2 f_K - m_\pi^2 f_\pi\right)}{\sqrt{2}} = 0\,, \tag{4.3}$$

with the notation introduced in (3.2).

Using (2.3), the requirement

$$\sigma_s(\infty) = 0\,, \quad \zeta_s(\infty) = 0$$

leads to the conditions

$$\begin{aligned} &\lambda^2\left(\frac{f_\pi^2}{2} + \frac{(2f_K - f_\pi)^2}{2} + \mu^2\right) = m_\pi^2\,, \\ &\lambda^2(2f_K - f_\pi)\left({f_\pi}^2 + \frac{(2f_K - f_\pi)^2}{2} + \mu^2\right) \\ &\quad = \left(2{m_K}^2 f_K - {m_\pi}^2 f_\pi\right)\,, \\ &\mu^2 = -1.29525\cdot 10^{-2}\ \mathrm{GeV}^2\,, \quad \lambda = 9.95484\,. \end{aligned} \tag{4.4}$$

As before [1] all meson functions were assumed to vanish at infinity. Generally speaking this means that

$$\tilde{\phi} \quad \to \quad \phi - \phi(\mathrm{VEV})\,, \quad \phi(\infty) \to 0\,. \tag{4.5}$$

**Table 1.** The quark–meson dimensionless coupling constants

| $g_M$ | $g_\sigma$ | $g_\pi$ | $g_K$ | $g_\eta$ | $g_{\eta'}$ | $g_{a_0}$ | $g_\kappa$ | $g_\zeta$ |
|---|---|---|---|---|---|---|---|---|
| | 10.7 | 4.0 | 7.8 | 4.0 | 3.1 | 1.5 | 3.9 | 10.5 |

Here for some fields $\phi(\mathrm{VEV}) = 0$. The coupling constants $g_M$ ($M = \eta, \pi, \ldots$) in (2.2) are connected with the linear boundary conditions (A2) which in the leading order in TDIA give the set (3.4). This cannot be satisfied by an universal coupling constant $g$ which figures in (2.2) and one encounters, as it was found before [1], some dynamical symmetry breaking. In the beginning of the numerical procedure one has to introduce some reasonable $g_M$ values. In the same way one also starts with the usual values for $\omega_0$ and $\omega_m$ [1]. After the meson fields (their profile functions) have been determined, one introduces that into the linear boundary conditions (3.4) which determine the coupling constants $g_M$. The new values of $g_M$ are used in solving the system of the non-linear differential equations (3.1) and the derivative boundary conditions (3.3). Such a self-consistent procedure is repeated (usually about 5000 times) until full agreement up to the prescribed tolerance is achieved. The stability of the system depends on the values $\omega_0$ and $\omega_m$ which are changed accordingly during iterations. The $U(3)\times U(3)$ model determines all coupling constants $g_M$ leading to the values shown in Table 1.

In the earlier approximations [1, 21] they were either overdetermined, or undetermined, so one had to revert to some educated guesses. The situation is presented in the following table, Table 2. Thus it seems that only the $U(3)\times U(3)$ model provides a fully self-consistent picture. If one started with some foolish initial values, say $g_\pi = 10^3$, a larger number of already mentioned iterations would lead to the results shown in Table 4.1. The model $g_\pi$ value is, interestingly, close to the estimated value in [17]. The corresponding $\omega$ values are

$$\omega_0 = 2.0; \quad \omega_m = 2.28\,. \tag{4.6}$$

In Fig. 2 the radial dependencies of $r^2\phi^2(r)$ ($\phi = \pi_p$, $K_p$, $\sigma_s$, $a_{0,s}$) are plotted. As can be seen from Figs. 1 and 2 the function corresponding to scalar fields ($r^2\sigma_s^2$, $r^2 a_{0,s}^2$) are much smaller than the contributions associated with pseudoscalars ($\pi_p$ and $K_p$). The smallness of the scalar contributions seems to agree with the baryon–meson interaction being dominated by pseudoscalar mesons. Moreover the $\sigma_s$ presence seems to be better established than the $a_0$ presence.

**Table 2.** Determination of coupling constants

| Model | No. of diffrential equations | No. of coupling constants | No. of linear equations | Ref. |
|---|---|---|---|---|
| $U(2)$ | 3 | 3 | 4 | [1] |
| $U(2)\times U(2)$ | 6 | 6 | 4 | [20] |
| $U(3)\times U(3)$ | 13 | 8 | 8 | This work |

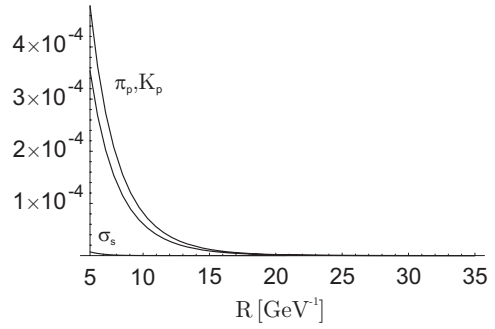


**Fig. 1.** Mesonic distributions $r^2\phi^2(r)$ outside the quark–meson boundary R ($R > 5\,\mathrm{GeV}^{-1}$)

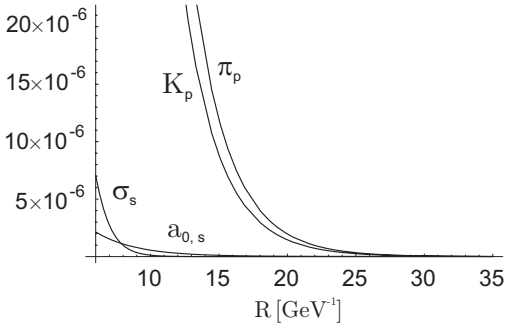


**Fig. 2.** Mesonic distributions $r^2\phi^2(r)$ outside the quark–meson boundary R ($R > 5\,\mathrm{GeV}^{-1}$), magnified

All model fields are described in the Furry bound state picture [22]. The field operators (2.6)–(2.9) are expanded in terms of the bound state fields (i.e. profile functions) which are solutions in the non-operator sense, of the system (see Sect. 3) of unquantized equations.

As one has solved the complex coupled system (3.1)–(3.5), which contains both non-strange and strange profile functions, one can say that $u$, $d$, $\pi$ etc. profile functions "feel" the presence of the $s$-quark dynamics.

## 5 Magnetic moments of the octet baryons

The general form of the model's vector current is

$$J^{\mu}_{\mathrm{EM},k} = J^{\mu}_{\mathrm{EM},Q} + J^{\mu}_{\mathrm{EM},M} \tag{5.1}$$
$$= : \bar{\psi}\gamma^{\mu}\frac{\lambda_k}{2}\psi + f_{klm}\left[\pi_l(\partial^{\mu}\pi_m) + \sigma_l(\partial^{\mu}\sigma_m)\right] : .$$

Its normalization is determined by the boundary conditions

$$\begin{aligned} -\mathrm{i}\gamma^{\mu}\hat{n}_{\mu}\psi &= g\left(\sigma_a + \mathrm{i}\pi_a\gamma_5\right)\lambda^a\psi\,, \\ (\partial^{\mu}\pi_m)\hat{n}_{\mu} &= -\frac{g}{2}\bar{\psi}\mathrm{i}\lambda_m\gamma_5\psi\,, \\ (\partial^{\mu}\sigma_m)\hat{n}_{\mu} &= -\frac{g}{2}\bar{\psi}\lambda_m\psi\,, \end{aligned} \tag{5.2}$$

which lead to

$$\hat{n}_{\mu}J^{\mu}_{\mathrm{EM},Q} = \hat{n}_{\mu}J^{\mu}_{\mathrm{EM},M} = -f_{klm}\bar{\psi}\frac{g}{2}(\sigma_l + \mathrm{i}\pi_l\gamma_5)\lambda_m\psi\,. \tag{5.3}$$

The quark and meson fields calculated in Sect. 4 are introduced in the expression for the magnetic moment [14, 23]:

$$\mu = \frac{1}{2}\langle B\uparrow|\int \mathrm{d}^3r\,(\mathbf{r}\times\mathbf{j}_{\mathrm{EM}})\,|B\uparrow\rangle\,. \tag{5.4}$$

Here $|B\uparrow\rangle$ are the usual octet baryon states [14, 15]. The quark contribution to the magnetic moment is

$$\mu^{(Q)} = \frac{1}{2}\langle B\uparrow|\int_0^{R_{\mathrm{bag}}}\mathrm{d}^3r\;\mathbf{r} \times\left[\bar{\psi}\left(\frac{1}{2}\lambda_3 + \frac{1}{2\sqrt{3}}\lambda_8\right)\gamma^{\mu}\psi\right]|B\uparrow\rangle\,. \tag{5.5}$$

For example the quark contribution to the magnetic moment for the proton is

$$\mu_p^{(Q)} = \frac{1}{2}\langle p\uparrow|\int_0^{R_{\mathrm{bag}}}\mathrm{d}^3r\;\mathbf{r} \times\left[\frac{2}{3}\bar{\psi}_u\gamma^{\mu}\psi_u - \frac{1}{3}\bar{\psi}_d\gamma^{\mu}\psi_d - \frac{1}{3}\bar{\psi}_s\gamma^{\mu}\psi_s\right]|p\uparrow\rangle\,, \tag{5.6}$$

$$\mu_p^{(Q)} = \frac{2}{3}\cdot\frac{R}{\omega^4} \times\frac{(\omega/2) - (3/8)\sin 2\omega + (\omega/4)\cos 2\omega}{j_0^2(\omega) + j_1^2(\omega) - 2j_0(\omega)j_1(\omega)/\omega}\,. \tag{5.7}$$

The proton state vector is listed in Appendix C.

Formally it looks like a standard bag model result [14, 15,23]. However the quark radial functions $f_0$, $g_0$ etc. satisfy the model system of equations which was given in Sect. 3. Thus $\omega_0(\omega_m)$ has the value (4.6).

The meson contribution is determined by meson solitons (i.e. the respective $s$- or $p$-states in (2.8) and (2.9)):

$$\mu^{(M)} = \frac{1}{2}\langle B\uparrow|\int_{R_{\mathrm{bag}}}^{\infty}\mathrm{d}^3r\,(\mathbf{r}\times\mathbf{J}_{\mathrm{EM},M})_z\,|B\uparrow\rangle\,. \tag{5.8}$$

The meson vector current appearing in (5.1) can be written as

$$\begin{aligned} J^{\mu}_{\mathrm{EM},M} =: &\,\mathrm{i}(\pi^+\partial^{\mu}\pi^- - \pi^-\partial^{\mu}\pi^+) \\ &+\mathrm{i}(K^+\partial^{\mu}K^- - K^-\partial^{\mu}K^+) + \mathrm{i}(a_0^+\partial^{\mu}a_0^- - a_0^-\partial^{\mu}a_0^+) \\ &+\mathrm{i}(\kappa^+\partial^{\mu}\kappa^- - \kappa^-\partial^{\mu}\kappa^+) : . \end{aligned} \tag{5.9}$$

Thus the meson contribution to the magnetic moment has the form

$$\mu^{(M)} = \frac{1}{2}\langle B\uparrow|\int_{R_{\mathrm{bag}}}^{\infty}\mathrm{d}^3r\left\{\mathbf{r}\times:\left[\mathrm{i}\phi^a(r)\chi^{\mu'\dagger}_{1/2}\,(\sigma\cdot\hat{r})\,\chi^{\mu}_{1/2}b^{a\dagger}_{\mu'}b^a_{\mu}\right] \times\nabla\left[\phi^b(r)\chi^{\nu'\dagger}_{1/2}\,(\sigma\cdot\hat{r})\,\chi^{\nu}_{1/2}b^{b\dagger}_{\nu'}b^b_{\nu}\right]:\right\}|B\uparrow\rangle\,. \tag{5.10}$$

Here $\phi^a$ refer to the meson operators $\pi^+$, $K^+$ etc. appearing in (5.9). Using the identities

$$\chi^{\mu'\dagger}_{1/2}\,(\sigma\cdot\hat{r})\,\chi^{\mu}_{1/2} = \sqrt{4\pi}\sum_{\alpha}C^{1/2\,\mu'}_{1\,-\alpha;1/2\,\mu}Y_1^{\alpha}(-1)^{\alpha+1}\,,$$

$$(\mathbf{r}\times\nabla)_z = \mathrm{i}L_z\,, \tag{5.11}$$

one arrives at the compact form

$$\mu^{(M)} = -4\pi \sum_{a,b,\alpha} C^{1/2\,\mu'}_{1\,-\alpha;1/2\,\mu} C^{1/2\,\nu'}_{1\,\alpha;1/2\,\nu}(-\alpha)(-1)^{\alpha} \times \langle B\uparrow| : \left[\frac{1}{2}\int_{R_{\rm bag}}^{\infty} r^2\mathrm{d}r\ \ \phi^a(r)\phi^b(r)\right] : |B\uparrow\rangle\,. \tag{5.12a}$$

Here the summation goes over all flavors appearing in (5.10). The quantities $\phi^a$ are the products of profile functions and operators from (2.8). For example

$$\phi^1(r) = \pi_p^+(r) b^{c\dagger}_{\mu',d} b^c_{\mu,u}\,. \tag{5.12b}$$

Spin indices denoted by Greek letters are used only in general expressions and the connection with our meson functions is the following:

$$m \Leftrightarrow \mu'\,, \quad m' \Leftrightarrow \mu\,, \quad n' \Leftrightarrow \nu\,, \quad n \Leftrightarrow \nu'\,.$$

It is immediately obvious from (5.10) and (5.11) that the scalar fields $a_0$, $\kappa$, ... do not contribute. When one employs the baryon wave functions [14,15] one has to evaluate matrix elements of the combinations containing 10 quark operators. For example

$$\begin{aligned}
&\pi^-\pi^+ \sim -u^{A\dagger}_m d^{B\dagger}_n d^A_{m'} u^B_{n'},\\
&\langle p\uparrow|(-\pi^-\pi^+)|p\uparrow\rangle\\
&= \frac{\varepsilon^{abc}\varepsilon^{\bar a\bar b\bar c}}{18}\Big\{\langle 0|u^{\bar c}_\uparrow d^{\bar b}_\uparrow u^{\bar a}_\downarrow u^{A\dagger}_m d^{B\dagger}_n d^A_{m'} u^B_{n'} u^{a\dagger}_\downarrow d^{b\dagger}_\uparrow u^{c\dagger}_\uparrow|0\rangle\\
&\quad -\langle 0|u^{\bar c}_\uparrow d^{\bar b}_\downarrow u^{\bar a}_\uparrow u^{A\dagger}_m d^{B\dagger}_n d^A_{m'} u^B_{n'} u^{a\dagger}_\uparrow d^{b\dagger}_\downarrow u^{c\dagger}_\uparrow|0\rangle\\
&\quad -\langle 0|u^{\bar c}_\uparrow d^{\bar b}_\downarrow u^{\bar a}_\uparrow u^{A\dagger}_m d^{B\dagger}_n d^A_{m'} u^B_{n'} u^{a\dagger}_\downarrow d^{b\dagger}_\uparrow u^{c\dagger}_\uparrow|0\rangle\\
&\quad +\langle 0|u^{\bar c}_\uparrow d^{\bar b}_\downarrow u^{\bar a}_\uparrow u^{A\dagger}_m d^{B\dagger}_n d^A_{m'} u^B_{n'} u^{a\dagger}_\uparrow d^{b\dagger}_\downarrow u^{c\dagger}_\uparrow|0\rangle\Big\}\,.
\end{aligned} \tag{5.13}$$

Here the shorthand notation $u^c_\uparrow = b^c_{u\uparrow}$ etc. was used. A simple program takes care of the evaluations of the expressions like (5.13). After the C-G coefficients from (5.12a) are calculated one finds for the proton

$$\begin{aligned}
\mu_p^{(M)} &= \frac{1}{2}\frac{8\pi}{3}\\
&\quad\times\left\{\int_{R_{\rm bag}}^{\infty} r^2\mathrm{d}r\pi_p^+(r)\pi_p^-(r) + \int_{R_{\rm bag}}^{\infty} r^2\mathrm{d}r\pi_p^-(r)\pi_p^+(r)\right\}\\
&= \frac{8\pi}{3}\int_{R_{\rm bag}}^{\infty} r^2\mathrm{d}r\ \ \pi_p^2(r)\,.
\end{aligned} \tag{5.14}$$

An earlier result [23], based on the model which had many features in common with ours, was

$$\mu_p^{(M)} = \frac{4\pi}{3}\frac{11}{3}\int_{R_{\rm bag}}^{\infty} r^2\mathrm{d}r\ \ \pi_p^2(r)\,. \tag{5.15}$$

As explained in Appendix C this difference is connected with the fact that we are using field operators (2.8) for mesons. Those operators appear in (5.10) in normal ordering.

In the same way one can calculate magnetic moments for all octet baryons. The results are presented in the last section below. The ones corresponding to the "'semiclassical" alternative (5.15) can be found in Appendix C.

## 6 Axial vector coupling constants

The axial-vector coupling constants $g_A^0$ and $g_A^k$ ($k = 1, 2, \ldots, 8$) are determined by the matrix elements of the axial-vector currents at this level of approximation:

$$\begin{aligned}
J_k^{5\mu} &= \bar\psi\gamma^\mu\gamma_5\frac{\lambda_k}{2}\psi\\
&\quad - \sqrt{\frac{2}{3}}\left[(\partial^\mu\sigma_0)\pi_k - \sigma_0(\partial^\mu\pi_k) + (\partial^\mu\sigma_k)\pi_0 - \sigma_k(\partial^\mu\pi_0)\right]\\
&\quad - d_{klm}\left[(\partial^\mu\sigma_l)\pi_m - \sigma_l(\partial^\mu\pi_m)\right]\,,\\
&\quad k,l,m = 1,2,\ldots,8\,,
\end{aligned} \tag{6.1}$$

and

$$\begin{aligned}
J_0^{5\mu} &= \bar\psi\gamma^\mu\gamma_5\frac{1}{2}\psi - \left[(\partial^\mu\sigma_a)\pi_a - \sigma_a(\partial^\mu\pi_a)\right],\\
&\quad a = 0,\ldots,8\,.
\end{aligned} \tag{6.2}$$

One calculates the matrix element

$$g_A^n = \langle B\uparrow|\int \mathrm{d}^3\mathbf{r} J_n^{5,3}(\mathbf{r})\,|\tilde B\uparrow\rangle\,, \quad n = 0,\ldots,8\,. \tag{6.3}$$

The procedure is entirely analogous to the one used to calculate the magnetic moments in the preceding section. (For example the meson part analogous to (5.13) contains matrix elements of 10 quark operators.) The final expression contains the quark ($Q$) and the mesonic ($M$) pieces, i.e.

$$g_A^n = g_{A,Q}^n + g_{A,M}^n\,, \tag{6.4}$$

where more properly one should have written $g^n_{A,M}(q^2=0)$ for example. This is the consequence of TDIA at the zeroth level as explained in introduction (see [1] also).

With $B = \tilde B = p$ one finds

$$g^0_{A,Q} = \frac{1}{3}\frac{j_0^2(\omega_0)+j_1^2(\omega_0)}{j_0^2(\omega_0)+j_1^2(\omega_0)-2j_0(\omega_0)j_1(\omega_0)/\omega_0}\,, \tag{6.5a}$$

$$\begin{aligned}
g^0_{A,M} &= 2\frac{4\pi}{3}\left\{\int_{R_{\rm bag}}^{\infty}\mathrm{d}^3r\ \ [\eta_p(r)\sigma_s'(r)(\sigma_s(r)-f_\pi)\mathcal{D}\eta_p(r)]\right.\\
&\quad\left. + \frac{1}{3}\int_{R_{\rm bag}}^{\infty}\mathrm{d}^3r\ \ [\pi_p(r)a^{0\,\prime}_{0,s}(r) - a^0_{0,s}(r)\mathcal{D}\pi_p(r)]\right\}\,,
\end{aligned} \tag{6.5b}$$

$$g^3_{A,Q} = \frac{5}{3}\frac{1}{3}\frac{j_0^2(\omega_0)+j_1^2(\omega_0)}{j_0^2(\omega_0)+j_1^2(\omega_0)-2j_0(\omega_0)j_1(\omega_0)/\omega_0} \tag{6.6a}$$

$$g^3_{A,M} = 2\frac{4\pi}{3}\left\{\frac{5}{3}\right. \tag{6.6b}$$
$$\times\int_{R_{\rm bag}}^{\infty}\mathrm{d}^3r\ [\pi_p(r)\sigma_s'(r)-(\sigma_s(r)-f_\pi)\mathcal{D}\pi_p(r)]$$
$$\left.-\frac{1}{3}\int_{R_{\rm bag}}^{\infty}\mathrm{d}^3r\ \left[\eta_p(r)a^{0\,\prime}_{0,s}(r)-a^0_{0,s}(r)\mathcal{D}\eta_p(r)\right]\right\},$$

$$g^8_{A,Q} = \frac{1}{3}\,\frac{j_0^2(\omega_0)+j_1^2(\omega_0)}{j_0^2(\omega_0)+j_1^2(\omega_0)-2j_0(\omega_0)j_1(\omega_0)/\omega_0}\,, \tag{6.7a}$$

$$g^8_{A,M} = 2\frac{4\pi}{3} \tag{6.7b}$$
$$\times\left\{\int_{R_{\rm bag}}^{\infty}\mathrm{d}^3r\ [\eta_p(r)\sigma_s'(r)-(\sigma_s(r)-f_\pi)\mathcal{D}\eta_p(r)]\right.$$
$$\left.+\frac{1}{3}\int_{R_{\rm bag}}^{\infty}\mathrm{d}^3r\ \left[\pi_p(r)a^{0\,\prime}_{0,s}(r)-a^0_{0,s}(r)\mathcal{D}\pi_p(r)\right]\right\},$$

with $\mathcal{D}=\mathrm{d}/\mathrm{d}r+2/r$.

The matrix elements of the strangeness changing PCACs, which appear in the semileptonic decays, lead to similar expressions. The quark contributions have the general form

$$J^{5,3}_{4+\mathrm{i}5,Q} = \langle B|\bar\psi\gamma^3\gamma_5\frac{1}{2}(\lambda_4+\mathrm{i}\lambda_5)\psi|B'\rangle\,,$$
$$(g_A)_{B,Q} = \langle B|u_m^{A\dagger}s_n^A|B'\rangle N_0N_m \tag{6.8a}$$
$$\times\left\{\int_0^R r^2\mathrm{d}r\ \left[\sqrt{1+\frac{m_s}{E}}\,j_0(\omega_m)j_0(\omega_0)\right]\right.$$
$$\left.-\frac{1}{3}\int_0^R r^2\mathrm{d}r\ \left[\sqrt{1-\frac{m_s}{E}}\,j_1(\omega_m)j_1(\omega_0)\right]\right\}.$$

The baryon states are as follows:

$$B=p\,,\quad B'=\Lambda\,,\quad B=n\,,$$
$$B'=\Sigma^-\quad B=\Lambda\,,\quad B'=\Xi^-\,. \tag{6.8b}$$

The corresponding mesonic parts are for $\Lambda\to p+e^-+\bar\nu_e$

$$(g_A)_M = -\frac{4\pi}{3\sqrt{6}}$$
$$\times\left\{3\int_{R_{\rm bag}}^{\infty}\mathrm{d}^3r\ [K_p(r)\sigma_s'(r)\right.$$
$$-(\sigma_s(r)-f_\pi)\mathcal{D}K_p(r)] \tag{6.9}$$
$$-\int_{R_{\rm bag}}^{\infty}\mathrm{d}^3r\ [\eta_p(r)\kappa_s'(r)-\kappa_s(r)\mathcal{D}\eta_p(r)]$$
$$\left.\times 2\int_{R_{\rm bag}}^{\infty}\mathrm{d}^3r\ [\pi_p(r)\kappa_s'(r)-\kappa_s(r)\mathcal{D}\pi_p(r)]\right\};$$

for $\Sigma^-\to n+e^-+\bar\nu_e$

$$(g_A)_M = -\frac{4\pi}{9}$$
$$\times\left\{\int_{R_{\rm bag}}^{\infty}\mathrm{d}^3r\ [K_p(r)\sigma_s'(r)\right.$$
$$-(\sigma_s(r)-f_\pi)\mathcal{D}K_p(r)] \tag{6.10}$$
$$-2\int_{R_{\rm bag}}^{\infty}\mathrm{d}^3r\ [\eta_p(r)\kappa_s'(r)-\kappa_s(r)\mathcal{D}\eta_p(r)]$$
$$-2\int_{R_{\rm bag}}^{\infty}\mathrm{d}^3r\ \left[K_p(r)a_{0,s}'(r)-a_{0,s}(r)\mathcal{D}K_p(r)\right]$$
$$\left.+\int_{R_{\rm bag}}^{\infty}\mathrm{d}^3r\ [\pi_p(r)\kappa_s'(r)-\kappa_s(r)\mathcal{D}\pi_p(r)]\right\};$$

for $\Xi^-\to\Lambda+e^-+\bar\nu_e$

$$(g_A)_M = -\frac{4\pi}{6\sqrt{6}}$$
$$\times\left\{\int_{R_{\rm bag}}^{\infty}\mathrm{d}^3r\ [K_p(r)\sigma_s'(r)\right.$$
$$-(\sigma_s(r)-f_\pi)\mathcal{D}K_p(r)]$$
$$-\int_{R_{\rm bag}}^{\infty}\mathrm{d}^3r\ [\eta_p(r)\kappa_s'(r)-\kappa_s(r)\mathcal{D}\eta_p(r)]$$
$$-3\int_{R_{\rm bag}}^{\infty}\mathrm{d}^3r\ \left[K_p(r)a_{0,s}'(r)-a_{0,s}(r)\mathcal{D}K_p(r)\right]$$
$$+2\int_{R_{\rm bag}}^{\infty}\mathrm{d}^3r\ [K_p(r)\zeta_s'(r)$$
$$-(\zeta_s(r)-\zeta_{\rm vac})\,\mathcal{D}K_p(r)]$$
$$+6\int_{R_{\rm bag}}^{\infty}\mathrm{d}^3r\ \left[\eta_p'(r)\kappa_s'(r)-\kappa_s(r)\mathcal{D}\eta_p'(r)\right] \tag{6.11}$$
$$\left.+3\int_{R_{\rm bag}}^{\infty}\mathrm{d}^3r\ [\pi_p(r)\kappa_s'(r)\quad-\kappa_s(r)\mathcal{D}\pi_p(r)]\right\}.$$

The corresponding numerical results can be found in the next section.

## 7 Results and conclusions

Our model formalism in TDIA at the lowest level of approximation is used for the evaluation of the magnetic moments and the axial-vector coupling constants of the non-strange and strange baryons.

The baryon magnetic moments are determined by quark $\mu^{(Q)}$ and meson $\mu^{(M)}$ pieces. As the flavor $SU(3)$ is broken only by $m_s\neq 0$, the quark piece has a contribution coming from the $u$, $d$ quarks $\mu_0^{(Q)}$ and a contribution coming from

the $s$ quark $\mu_s^{(Q)}$. The meson pieces depend on the pion soliton $\mu_\pi^{(M)}$ and the kaon soliton $\mu_K^{(M)}$. Their values are

$$\mu_0^{(Q)} = 1.886\,, \quad \mu_s^{(Q)} = 1.695\,, \tag{7.1}$$

$$\mu_\pi^{(M)} = \frac{8\pi}{3}\int_{R_{\rm bag}}^{\infty} r^2 {\rm d}r\ \pi_p^2(r) = 0.027\,, \tag{7.2a}$$

$$\mu_K^{(M)} = \frac{8\pi}{3}\int_{R_{\rm bag}}^{\infty} r^2 {\rm d}r\ K_p^2(r) = 0.020\,. \tag{7.2b}$$

The full expressions $\mu_B = \mu_B^Q + \mu_B^M$ are

$$\mu_p = \mu_0^Q + \mu_\pi^M\,, \tag{7.3a}$$

$$\mu_n = -\frac{2}{3}\mu_0^Q - \mu_\pi^M\,, \tag{7.3b}$$

$$\mu_\Lambda = -\frac{1}{3}\mu_s^Q - \mu_K^M\,, \tag{7.3c}$$

$$\mu_{\Sigma^0} = \frac{2}{9}\mu_0^Q + \frac{1}{9}\mu_s^Q + \frac{1}{2}\mu_K^M\,, \tag{7.3d}$$

$$\mu_{\Sigma^+} = \frac{8}{9}\mu_0^Q + \frac{1}{9}\mu_s^Q + \mu_K^M\,, \tag{7.3e}$$

$$\mu_{\Sigma^-} = -\frac{4}{9}\mu_0^Q + \frac{1}{9}\mu_s^Q\,, \tag{7.3f}$$

$$\mu_{\Sigma^0\Lambda} = \frac{1}{\sqrt{3}}\mu_0^Q + \frac{1}{\sqrt{3}}\left(\mu_\pi^M + \frac{1}{2}\mu_K^M\right), \tag{7.3g}$$

$$\mu_{\Xi^0} = -\frac{2}{9}\mu_0^Q - \frac{4}{9}\mu_s^Q - \mu_K^M\,, \tag{7.3h}$$

$$\mu_{\Xi^-} = \frac{1}{9}\mu_0^Q - \frac{4}{9}\mu_s^Q\,. \tag{7.3i}$$

In Table 3 the model values are compared with experimental results. Signs are predicted correctly, but overall agreement is not satisfactory although at this level of approximation where no other refinement of the models is applied one can be quite pleased with the results. Moreover the predicted value does not depend on the details of the model as shown in Table 4.

Although both quark $Q$ and meson $M$ phases were calculated in a model which includes $s$ quarks, only the simplest "valence" proton state vectors (C2) were used.

**Table 3.** Baryon magnetic moments

| Baryon | $\mu_Q$ | $\mu_M$ | $\mu$ | $\mu_{\rm exp}$ | $\Delta\mu$ % |
|---|---|---|---|---|---|
| $p$ | 1.886 | 0.027 | 1.913 | 2.793 | 46 |
| $n$ | −1.257 | −0.026 | −1.284 | −1.913 | 49 |
| $\Lambda$ | −0.564 | −0.020 | −0.584 | −0.613 | 8 |
| $\Sigma^0$ | 0.607 | 0.010 | 0.617 | – | – |
| $\Sigma^0 \to \Lambda$ | 1.089 | 0.021 | 1.110 | 1.610 | 45 |
| $\Sigma^-$ | −0.650 | 0.000 | −0.650 | −1.160 | 78 |
| $\Sigma^+$ | 1.864 | 0.020 | 1.884 | 2.458 | 31 |
| $\Xi^0$ | −1.172 | −0.020 | −1.191 | −1.250 | 5 |
| $\Xi^-$ | −0.543 | 0.000 | −0.543 | −0.651 | 20 |

**Table 4.** Proton magnetic moment

| Model | $\mu_Q$ | $\mu_M$ | $\mu$ | Ref. |
|---|---|---|---|---|
| $U(2)$ | 1.886 | 0.037 | 1.923 | [1] |
| $U(2)\times U(2)$ | 1.886 | 0.018 | 1.904 | [21] |
| $U(3)\times U(3)$ | 1.886 | 0.027 | 1.913 | This work |

**Table 5.** Diagonal axial-vector constants

| Constant | $g_A^{(Q)}$ | $g_A^{(M)}$ | $g_A$ | Experiment | $\Delta g$ % |
|---|---|---|---|---|---|
| $g_A^3$ | 1.110 | 0.184 | 1.294 | 1.267 | 2 |
| $g_A^0$ | 0.666 | 0.111 | 0.777 | 0.280 | 178 |
| $g_A^8$ | 0.666 | 0.111 | 0.777 | 0.579 | 34 |

**Table 6.** $g_A^3$ calculated in various non-linear models

| Model | $g_{A,Q}^3$ | $g_{A,M}^3$ | $g_A^3$ | Ref. | $\Delta g$ % |
|---|---|---|---|---|---|
| $U(2)$ | 1.110 | 0.146 | 1.246 | [1] | 1 |
| $U(2)\times U(2)$ | 1.110 | 0.146 | 1.246 | [21] | 1 |
| $U(3)\times U(3)$ | 1.110 | 0.184 | 1.294 | This work | 2 |

The same "valence" approximation [14, 15] was used for the other baryon state vectors so this is precisely the place where one could start refining the model. This should be (and will be) done because this would invoke the strange component in the proton without which one cannot address the problem of the axial anomaly or nucleon strange form factors.

The $s$-quark admixture in the non-strange baryon state vectors would pick up additional contributions from quark and meson fields calculated in TDIA. That would change both the theoretical expressions for the magnetic moments and for the axial-vector coupling constants. However, from the point of view of the present work, that would require a substantial addition to the model.

A very similar conclusion follows from the investigation of the axial-vector coupling constants. The evaluation of the "diagonal" cases (6.5), (6.6) and (6.7) are summarized in Table 5. It seems reasonable to assume that the discrepancies are again caused by the too poor structure of the proton state vectors. It is usually stated [16] that $s$ quark admixture in the proton state vector must be important. However, the prediction for the isovector axial-vector coupling constant $g_A^3$ is very good. This seems to be some general characteristic of the chiral models which are constructed to satisfactory reproduce $g_A^{I=1}$. Moreover the present non-linear, non-perturbative approach seems to work somewhat better than some simple expansions which might lead to too large $g_A^{I=1}$.

The enlarged $U(3)\times U(3)$ model seems to predict somewhat worse values for $g_A^3$ than earlier attempts. However, the results shown in Table 6 are not significantly different. The present value is about 3% too large. The $g_A^0$ values are more model dependent, as seen in Table 7. The small difference shown there is due to symmetry breaking. In the $U(2)\times U(2)$ case [21] the $\pi$ and $\eta$ fields were non-degenerate. In the present approach the $\pi$ and $\eta$ are degenerate. That was done in order to limit the number of non-linear equations (see (2.2) and (3.1), and Appendix A)

**Table 7.** $g_A^0$ calculated in various non-linear models

| Model | $g_{A,Q}^0$ | $g_{A,M}^0$ | $g_A^0$ | Ref. |
|---|---|---|---|---|
| $U(2)\times U(2)$ | 0.666 | −0.008 | 0.658 | [20] |
| $U(3)\times U(3)$ | 0.666 | 0.111 | 0.777 | This work |

**Table 8.** $g_A$ in semileptonic decays

| Decay | $(g_A)_Q$ | $(g_A)_M$ | $g_A$ | exp. | $\Delta g$ % |
|---|---|---|---|---|---|
| $\Lambda \to p + e^- + \bar{\nu}_e$ | −0.758 | −0.059 | −0.817 | −0.718 | 14 |
| $\Sigma^- \to n + e^- + \bar{\nu}_e$ | 0.206 | 0.016 | 0.222 | 0.340 | 53 |
| $\Xi^- \to \Lambda + e^- + \bar{\nu}_e$ | −0.253 | −0.029 | −0.282 | −0.250 | 13 |

to some reasonable level. The differences in the symmetry breaking does not have a significant influence. The present value is only 18% larger than the older [21] estimate.

As shown in Table 8 the calculated $g_A$'s, for the semileptonic decays (6.9), (6.10) and (6.12), seem reasonable in the two cases. All signs are correctly predicted, the absolute magnitude of the $\Lambda$-decay constant is 14% too large, the $\Sigma$-decay constant is 53% too small and the $\Xi^-$-decay constant is 13% too large. One cannot learn more from those results than one has already learned from Table 5. Here, as in Tables 5–7 the meson phase contribution is noticeably smaller than the quark phase contributions. This might look as a support for the simple quark models [14,15]. However, our model, which contains the spherical cavity as an essential ingredient, might be biased in that direction. Thus in the future one should attempt to solve a model in which a quark bound state does not need a bag.

In its present form this non-linear self-consistent model shows interesting features. For example the $\pi$ and $K$ contributions (see Fig. 1) are considerably larger than the $\sigma$ and $a_0$ contribution. One is tempted to conclude that this reflects the fact that in baryonic processes the presence of scalars was hard to detect. Generally speaking the model offers stable and physically acceptable [9–11] solutions.

In this model the complete problem with $u$, $d$ and $s$ quarks and two meson nonets has been solved in TDIA. Quite complicated non-linear operator dynamics has been reduced to the highly non-trivial, but solvable, non-linear system.

All model dependent quantities, Tables 3–8, have acceptable orders of magnitude. All relative signs for $\mu$ and $g_A$ are correctly predicted. The discrepancies with the experimental magnitudes reflect the exploratory character of the present TDIA solution. They might be connectable to the too simple description of the baryon state vectors [16] and to the absence of exchange current corrections [17,25]. A future development of the TDIA based solution might lead to better predictions also in the context of multiquark states [26] built in the TDIA formalism.

## Appendix A

The equations of motion and boundary conditions for the quantum fields $a_0(x)$, $K^+(x)$, $\psi(x)$, ... are

$$\mathrm{i}\gamma^\mu \partial_\mu \psi = 0\,, \quad m_s = 0\,, \tag{A1}$$

$$-\mathrm{i}\gamma^\mu \hat{n}_\mu \psi|_{r=R} = g\left(\sigma_a + \mathrm{i}\pi_a\gamma_5\right)\lambda^a\psi|_{r=R}\,, \tag{A2}$$

$$\partial_\mu\partial^\mu a_0^- + \lambda^2 a_0^-\left(\sigma_a^2+\pi_a^2+\mu^2\right) = 0\,, \tag{A3}$$

$$\left(\partial^\mu a_0^-\right)\hat{n}_\mu = -\frac{g}{2}\overline{\psi}\lambda_{12}^-\psi\Big|_{r=R}\,, \tag{A4}$$

$$\partial_\mu\partial^\mu a_0^+ + \lambda^2 a_0^+\left(\sigma_a^2+\pi_a^2+\mu^2\right) = 0\,, \tag{A5}$$

$$\left(\partial^\mu a_0^+\right)\hat{n}_\mu = -\frac{g}{2}\overline{\psi}\lambda_{12}^+\psi\Big|_{r=R}\,, \tag{A6}$$

$$\partial_\mu\partial^\mu a_0^0 + \lambda^2 a_0^0\left(\sigma_a^2+\pi_a^2+\mu^2\right) = 0\,, \tag{A7}$$

$$\left(\partial^\mu a_0^0\right)\hat{n}_\mu = -\frac{g}{2}\overline{\psi}\lambda_3\psi\Big|_{r=R}\,, \tag{A8}$$

$$\partial_\mu\partial^\mu \kappa^+ + \lambda^2\kappa^+\left(\sigma_a^2+\pi_a^2+\mu^2\right) = 0\,, \tag{A9}$$

$$\left(\partial^\mu \kappa^+\right)\hat{n}_\mu = -\frac{g}{2}\overline{\psi}\lambda_{45}^+\psi\Big|_{r=R}\,, \tag{A10}$$

$$\partial_\mu\partial^\mu \kappa^- + \lambda^2\kappa^-\left(\sigma_a^2+\pi_a^2+\mu^2\right) = 0\,, \tag{A11}$$

$$\left(\partial^\mu \kappa^-\right)\hat{n}_\mu = -\frac{g}{2}\overline{\psi}\lambda_{45}^-\psi\Big|_{r=R}\,, \tag{A12}$$

$$\partial_\mu\partial^\mu \kappa^0 + \lambda^2\kappa^0\left(\sigma_a^2+\pi_a^2+\mu^2\right) = 0\,, \tag{A13}$$

$$\left(\partial^\mu \kappa^0\right)\hat{n}_\mu = -\frac{g}{2}\overline{\psi}\lambda_{67}^+\psi\Big|_{r=R}\,, \tag{A14}$$

$$\partial_\mu\partial^\mu \overline{\kappa^0} + \lambda^2\overline{\kappa^0}\left(\sigma_a^2+\pi_a^2+\mu^2\right) = 0\,, \tag{A15}$$

$$\left(\partial^\mu \overline{\kappa^0}\right)\hat{n}_\mu = -\frac{g}{2}\overline{\psi}\lambda_{67}^-\psi\Big|_{r=R}\,, \tag{A16}$$

$$\partial_\mu\partial^\mu \sigma + \lambda^2\sigma\left(\sigma_a^2+\pi_a^2+\mu^2\right) + m_\pi^2 f_\pi = 0\,, \tag{A17}$$

$$\left(\partial^\mu \sigma\right)\hat{n}_\mu = -\frac{g}{2}\overline{\psi}\lambda_{08}^-\psi\Big|_{r=R}\,, \tag{A18}$$

$$\partial_\mu\partial^\mu \zeta + \lambda^2\zeta\left(\sigma_a^2+\pi_a^2+\mu^2\right) = \frac{\left(m_\pi^2 f_\pi - 2m_K^2 f_K\right)}{\sqrt{2}}\,, \tag{A19}$$

$$\left(\partial^\mu \zeta\right)\hat{n}_\mu = -\frac{g}{2}\overline{\psi}\lambda_{08}^+\psi\Big|_{r=R}\,, \tag{A20}$$

$$\partial_\mu\partial^\mu \pi^- + \lambda^2\pi^-\left(\sigma_a^2+\pi_a^2+\mu^2\right) = 0\,, \tag{A21}$$

$$\left(\partial^\mu \pi^-\right)\hat{n}_\mu = -\frac{g}{2}\overline{\psi}\mathrm{i}\lambda_{12}^-\gamma_5\psi\Big|_{r=R}\,, \tag{A22}$$

$$\partial_\mu\partial^\mu \pi^+ + \lambda^2\pi^+\left(\sigma_a^2+\pi_a^2+\mu^2\right) = 0\,, \tag{A23}$$

$$\left(\partial^\mu \pi^+\right)\hat{n}_\mu = -\frac{g}{2}\overline{\psi}\mathrm{i}\lambda_{12}^+\gamma_5\psi\Big|_{r=R}\,, \tag{A24}$$

$$\partial_\mu\partial^\mu \pi^0 + \lambda^2\pi^0\left(\sigma_a^2+\pi_a^2+\mu^2\right) = 0\,, \tag{A25}$$

$$\left(\partial^\mu \pi^0\right)\hat{n}_\mu = -\frac{g}{2}\overline{\psi}\mathrm{i}\lambda_3\gamma_5\psi\Big|_{r=R}\,, \tag{A26}$$

$$\partial_\mu\partial^\mu K^+ + \lambda^2 K^+\left(\sigma_a^2+\pi_a^2+\mu^2\right) = 0\,, \tag{A27}$$

$$\left(\partial^\mu K^+\right)\hat{n}_\mu = -\frac{g}{2}\overline{\psi}\mathrm{i}\lambda_{45}^+\gamma_5\psi\Big|_{r=R}\,, \tag{A28}$$

$$\partial_\mu\partial^\mu K^- + \lambda^2 K^-\left(\sigma_a^2+\pi_a^2+\mu^2\right) = 0\,, \tag{A29}$$

$$\left(\partial^\mu K^-\right)\hat{n}_\mu = -\frac{g}{2}\overline{\psi}\mathrm{i}\lambda_{45}^-\gamma_5\psi\Big|_{r=R}\,, \tag{A30}$$

$$\partial_\mu\partial^\mu K^0 + \lambda^2 K^0\left(\sigma_a^2+\pi_a^2+\mu^2\right)=0\,, \tag{A31}$$

$$\left(\partial^\mu K^0\right)\hat{n}_\mu = -\frac{g}{2}\overline{\psi}\mathrm{i}\lambda_{67}^{+}\gamma_5\psi\Big|_{r=R}\,, \tag{A32}$$

$$\partial_\mu\partial^\mu \overline{K^0} + \lambda^2 \overline{K^0}\left(\sigma_a^2+\pi_a^2+\mu^2\right)=0\,, \tag{A33}$$

$$\left(\partial^\mu \overline{K^0}\right)\hat{n}_\mu = -\frac{g}{2}\overline{\psi}\mathrm{i}\lambda_{67}^{-}\gamma_5\psi\Big|_{r=R}\,, \tag{A34}$$

$$\partial_\mu\partial^\mu \eta + \lambda^2 \eta\left(\sigma_a^2+\pi_a^2+\mu^2\right)=0\,, \tag{A35}$$

$$\left(\partial^\mu \eta\right)\hat{n}_\mu = -\frac{g}{2}\overline{\psi}\mathrm{i}\lambda_{08}^{-}\gamma_5\psi\Big|_{r=R}\,, \tag{A36}$$

$$\partial_\mu\partial^\mu \eta' + \lambda^2 \eta'\left(\sigma_a^2+\pi_a^2+\mu^2\right)=0\,, \tag{A37}$$

$$\left(\partial^\mu \eta'\right)\hat{n}_\mu = -\frac{g}{2}\overline{\psi}\mathrm{i}\lambda_{08}^{+}\gamma_5\psi\Big|_{r=R} \tag{A38}$$

## Appendix B

The finite $s$-quark mass $m_s$ (2.7) plays a role in the numerical solutions of the complex system (3.1)–(3.4). From the model structure (2.1)–(2.3) one expects the divergence of an axial-vector current which is consistent with PCAC [2]. However the finite $s$-quark mass in the bag environment leads to a consistency question. For a $4+\mathrm{i}5$ component of an axial-vector current

$$\begin{aligned} J_k^{5\mu} = {} & \bar{\psi}\gamma^\mu\gamma_5\frac{\lambda_k}{2}\psi\Theta - \sqrt{\frac{2}{3}}\left[\left(\partial^\mu\sigma_0\right)\pi_k - \sigma_0\left(\partial^\mu\pi_k\right)\right]\bar{\Theta} \\ & + \sqrt{\frac{2}{3}}\left[\left(\partial^\mu\sigma_k\right)\pi_0 - \sigma_k\left(\partial^\mu\pi_0\right)\right. \\ & \left. - d_{klm}\left(\left(\partial^\mu\sigma_l\right)\pi_m - \sigma_l(\partial^\mu\pi_m)\right)\right]\bar{\Theta}\,, \\ & k,l,m = 0,1,\ldots,8\,, \end{aligned} \tag{B1}$$

one finds the following contributions inside ($\Theta \equiv \Theta(R)$) and outside ($\bar{\Theta} \equiv 1-\Theta(R)$) the quark–meson boundary:

$$\begin{aligned} \partial_\mu(J^{5\mu}_{Q,k})_{\mathrm{s-wave}} &= \frac{N_0 N_m}{4\pi}(f_m f_0 + g_m g_0)m_s\Big|_{\Theta}\,, \\ \partial_\mu(J^{5\mu}_{M,k})_{\mathrm{s-wave}} &= \sqrt{2}K_s(r)m_K^2 f_K\Big|_{\bar{\Theta}}\,, \\ \partial_\mu(J^{5\mu}_{Q,k})_{\mathrm{p-wave}} &= \frac{N_0 N_m}{4\pi}(f_m g_0 + g_m f_0)m_s\Big|_{\Theta}\,, \\ \partial_\mu(J^{5\mu}_{M,k})_{\mathrm{p-wave}} &= \sqrt{2}K_p(r)m_K^2 f_K\Big|_{\bar{\Theta}}\,, \\ k &= 4+\mathrm{i}5\,. \end{aligned} \tag{B2}$$

Outside this one has the canonical PCAC form [14,15,25]. Inside that can be expressed only via quark functions $f_i, g_j$. Although our model does not impose any direct conditions, it seems reasonable to expect that the outside and inside phase should be equal at the boundary, thus ensuring the validity of PCAC in the whole space. Indirectly this is also connected with the derivative conditions (A22)–(A38) and (3.3).

Introducing the model determined functions $f_m(R)$, $f_0(R)$, $g_m(R)$, $g_0(R)$, $K_s(R)$ and $K_p(R)$ and using (4.1) and (4.6) one finds a reasonable consistency. The corresponding pieces in (B2) are numerically equal, at $r=R$, within 9% accuracy. It should be also mentioned that $\omega_0$ and $\omega_m$ in (2.8) are not arbitrary parameters. As described in Sect. 4. their values are determined by the system (3.1), (3.3) and (3.4).

## Appendix C

Reference [23] has constructed the meson phase (soliton fields) as a continuation of quark densities. In our formalism their result [23] is reproduced if one does not employ the normally ordered electromagnetic current (5.1). In the present formalism the normal ordering leads [27,28] to the vanishing vacuum matrix element of the current (5.1).

Without normal ordering the pion field densities appearing in (5.13) can be written as

$$\begin{aligned} \pi^-\pi^+ &\sim u_m^{A\dagger} d_{m'}^A d_n^{B\dagger} u_{n'}^B \\ &= -u_m^{A\dagger} d_n^{B\dagger} d_{m'}^A u_{n'}^B + \delta^{AB}_{m',n} u_m^{A\dagger} u_{n'}^B\,, \\ \pi^+\pi^- &\sim d_m^{A\dagger} u_{m'}^A u_n^{B\dagger} d_{n'}^B \\ &= -d_m^{A\dagger} u_n^{B\dagger} u_{m'}^A d_{n'}^B + \delta^{AB}_{m',n} d_m^{A\dagger} d_{n'}^B\,. \end{aligned} \tag{C1}$$

The additional terms appearing in (C1) are sandwiched between proton state vectors:

$$\begin{aligned} |p\uparrow\rangle &= \frac{\varepsilon^{abc}}{\sqrt{18}}\left[u_\downarrow^{a\dagger} d_\uparrow^{b\dagger} u_\uparrow^{c\dagger} - u_\uparrow^{a\dagger} d_\downarrow^{b\dagger} u_\uparrow^{c\dagger}\right]|0\rangle\,, \\ \langle p\uparrow| &= \langle 0|\frac{\varepsilon^{\bar{a}\bar{b}\bar{c}}}{\sqrt{18}}\left[u_\uparrow^{\bar{c}} d_\uparrow^{\bar{b}} u_\downarrow^{\bar{a}} - u_\uparrow^{\bar{c}} d_\downarrow^{\bar{b}} u_\uparrow^{\bar{a}}\right]. \end{aligned} \tag{C2}$$

One finds

$$\begin{aligned} \langle p\uparrow|(\delta^{AB}_{\mu,\nu'} d_{\mu'}^{A\dagger} d_\nu^B)|p\uparrow\rangle &= \frac{2}{3}\delta_{\mu,\nu'}\delta_{\mu'\downarrow,\nu\downarrow} + \frac{1}{3}\delta_{\mu,\nu'}\delta_{\mu'\uparrow,\nu\uparrow}\,, \\ \langle p\uparrow|(\delta^{AB}_{\mu,\nu'} u_{\mu'}^{A\dagger} u_\nu^B)|p\uparrow\rangle &= \frac{1}{3}\delta_{\mu,\nu'}\delta_{\mu'\downarrow,\nu\downarrow} + \frac{5}{3}\delta_{\mu,\nu'}\delta_{\mu'\uparrow,\nu\uparrow}\,. \end{aligned} \tag{C3}$$

Using

$$\begin{aligned} \mu^{(M)} = {} & -4\pi\sum_{\mu,\alpha} C^{1/2\,\mu'}_{1\,-\alpha;1/2\,\mu} C^{1/2\,\mu}_{1\,\alpha;1/2\,\nu}(-\alpha)(-1)^\alpha \\ & \times\left[\frac{1}{2}\int_{R_{\mathrm{bag}}}^\infty r^2\mathrm{d}r\;\;\phi^a(r)\phi^b(r)\right], \end{aligned} \tag{C4}$$

one eventually arrives at the result

$$\frac{4\pi}{3}\cdot\frac{5}{3}\int_{R_{\mathrm{bag}}}^\infty r^2\mathrm{d}r\;\;\pi_p^2(r)\,. \tag{C5}$$

When this is added to the result (5.14) one obtains the value given by [23]

$$\mu_p^M = \frac{4\pi}{3}\cdot\left(2+\frac{5}{3}\right)\int_{R_{\mathrm{bag}}}^\infty r^2\mathrm{d}r\;\;\pi_p^2(r)$$

**Table 9.** Baryon magnetic moments

| Baryon | $\mu_Q$ | $\mu_M^{\rm TDIA}$ | $\mu^{\rm TDIA}$ | $\mu_M^{[22]}$ | $\mu^{[22]}$ | $\mu_{\rm exp}$ |
|---|---|---|---|---|---|---|
| $p$ | 1.886 | 0.027 | 1.913 | 0.050 | 1.936 | 2.793 |
| $n$ | −1.257 | −0.026 | −1.284 | −0.050 | −1.307 | −1.913 |
| $\Lambda$ | −0.564 | −0.020 | −0.584 | −0.030 | −0.594 | −0.613 |
| $\Sigma^0$ | 0.607 | 0.010 | 0.617 | 0.020 | 0.627 | – |
| $\Sigma^0 \to \Lambda$ | 1.089 | 0.021 | 1.110 | 0.043 | 1.132 | 1.610 |
| $\Sigma^-$ | −0.650 | 0.000 | −0.650 | −0.007 | −0.657 | −1.160 |
| $\Sigma^+$ | 1.864 | 0.020 | 1.884 | 0.037 | 1.901 | 2.458 |
| $\Xi^0$ | −1.172 | −0.020 | −1.191 | −0.031 | −1.203 | −1.250 |
| $\Xi^-$ | −0.543 | 0.000 | −0.543 | −0.004 | −0.547 | −0.651 |

$$= \frac{4\pi}{3} \cdot \frac{11}{3} \int_{R_{\rm bag}}^{\infty} r^2 {\rm d}r \;\; \pi_p^2(r)\,. \qquad \text{(C6)}$$

Using the TDIA model values for the profile functions $\pi_p$, $K_p$ etc. one does not find a significant numerical difference between the expressions (5.14) and (C6) as summarized in Table 9.

## References


1. D. Horvat, B. Podobnik, D. Tadić, Phys. Rev. D **58**, 034003 (1998)
2. J. Schwinger, Ann. Phys. **2**, 407 (1957); M. Gell-Mann, M. Lévi, Nuovo Cimento **16**, 705 (1960); B.W. Lee, Nucl. Phys. B **9**, 649 (1969); S. Gasiorowicz, D.A. Geffen Rev. Mod. Phys. **41**, 531 (1969); J. Schechter, Y. Ueda, Phys. Rev. D **3**, 2874 (1971); H. Pagels, Phys. Rep. C **16**, 218 (1975)
3. M. Lévi, Nuovo Cimento A **52**, 23 (1967)
4. T.H.R. Skyrme, Proc. Roy. Soc. London, **260**, 127 (1961); **262**, 237 (1961); Nucl. Phys. **31**, 550 (1962); G.S. Adkins, C.R. Nappi, E. Witten, Nucl. Phys. B **228**, 552 (1983), B **233**, 109 (1984); I. Zahed, G.E. Brown, Phys. Rep. **142**, 1 (1986)
5. A. Chodos, B.C. Thorn, Phys. Rev D **12**, 2733 (1975)
6. M.C. Birse, M.K. Banerjee, Phys. Lett. B **136**, 284 (1984); Phys. Rev. D **31**, 118 (1985); M.C. Birse, Phys. Rev D **33**, 1934 (1986)
7. J.A. McGovern, M.C. Birse, Phys Lett. B **200**, 401 (1987); Nucl. Phys. A **506**, 367 (1990); A **506**, 393 (1990); Fizika 19, Suppl. **2**, 56 (1987)
8. I. Tamm, J. Phys. (Moscow) **9**, 449 (1945); S.M. Dancoff, Phys. Rev. **78**, 382 (1950)
9. N.A. Törnqvist, Phys. Rev. Lett. **49**, 624 (1982); Z. Phys. C **68**, 647 (1995)
10. N.A. Törnqvist, Phys. Rev. Lett. **76**, 1575 (1996)
11. N.A. Törnqvist, Phys. Lett. B **426**, 105 (1998); hep-ph/9905282 (1999); hep-ph/9910443 (1999)
12. G. Källen, Quantum electrodynamics (Springer-Verlag, New York-Heidelberg-Berlin 1972)
13. A.W. Thomas, Adv. Nucl. Physics 13, 1, edited by J.W. Negele, E. Vogt (Plenum, New York, 1984), Vol. 13, p. 1; G.E. Brown, M. Rho, Phys. Lett. B **82**, 177 (1979); G.E. Brown, M. Rho, V. Vento, Phys. Lett. B **84**, 383 (1979); H. Hogaasen, F. Myhrer, Z. Phys. C **73** 21 (1983); Xue-Qian Li, Zhen Qi, Commun. Theor. Phys. **213**, 18 (1992); G.E. Brown, M. Rho, Comments on Nucl. Part. Phys. **1**, 18 (1988); F. Myhrer, in Quarks and Nuclei, Vol. 1 of International Review of Nuclear Physics, edited by W. Weise (World Scientific, Singapore 1984); A. Hosaka, H. Toki, Phys. Rep. **65**, 277 (1996)
14. U. Mosel: Fields, symmetries and quarks (McGraw-Hill, Hamburg 1988)
15. J.F. Donoghue, E. Golowich, B.R. Holstein: Dynamics of the standard model (Cambridge University Press, Cambridge 1992)
16. J.F. Donoghue, E. Golowich, Phys. Lett. B **69**, 4337 (1977); Phys. Rev. D **15**, 3421 (1977); V. Sanjose, V. Vento, FTUV/88-29,IFIC/88-12 (1988); C.H. Chang, J.G. Hu, C.S. Huang, X.Q. Li, AS-ITP-90-25 (1991); H.W. Hammer, D. Drechsel, T. Mart, nucl-th/9701008 (1997); H.J. Lee, D.P. Min, B.Y. Park, M. Rho, V. Vento, Nucl. Phys. A **657**, 75 (1999); B.Q. Ma, I. Schmidt, J.J. Yang, Eur. Phys. J. A **12**, 353 (2001); S.D. Bass, hep-ph/0210214 (2002)
17. L.Ya. Glozman, D.O. Riska, Phys. Rept. **268**, 263 (1996); K. Tsushima, D.O. Riska, P.G. Blunden, Nucl. Phys. A **559**, 543 (1993); C. Helminen, K. Dannbom, D.O. Riska, L.Y. Glozman, Nucl. Phys. A **616**, 555 (1997); D.O. Riska, Few Body Syst. Suppl. **10**, 415 (1999); L. Hannelius, D.O. Riska, L.Y. Glozman, Nucl. Phys. A **665**, 353 (2000); L. Hannelius, D.O. Riska, Phys. Rev. C **62**, 045204 (2000)
18. G. Ripka, Quarks bound by chiral fields (Claredon Press, Oxford 1997)
19. M. Fiolhais, J.N. Urbano, K. Goeke, Phys. Lett. B **150**, 253 (1985); K. Goeke, M. Fiolhais, J.N. Urbano, M. Harvey, B **164**, 249 (1985); E. Ruiz Arriola, P. Alberto, J.N. Urbano, K. Goeke, Z. Phys. A **333**, 203 (1989); T. Nauber, M. Fiolhais, K. Goeke, J.N. Urbano, Nucl. Phys. A **560**, 909 (1993)
20. U. Ascher, J. Christiansen, R.D. Russel, Math. Comp. **33**, 659 (1979); ACM Trans. Math. Software **7**, 209 (1981); SIAM (Soc. Ind. Appl. Math.) Rev. **23**, 238 (1981)
21. D. Horvat, D. Horvatić, B. Podobnik, D. Tadić, Fizika B **9**, 181 (2000)
22. S.S. Schweber: An introduction to relativistic quantum field theory (Row, Peterson, Co., Evanson 1961)
23. M.V. Barnhill III, A. Halprin, Phys. Rev. D **21**, 1961 (1980)
24. K. Hagiwara et al., Phys. Rev. D **66**, 010001 (2002)
25. S.L. Adler, R.F. Dashen, Current algebras (W.A. Benjamin, Inc., New York, Amsterdam 1968)
26. C. Amsler, N.A. Tornqvist, Phys. Rept. **389**, 61 (2004)
27. J.D. Bjorken, S.D. Drell, Relativistic quantum fields (McGraw Hill, New York 1965)
28. S. Weinberg, The quantum theory of fields (Cambridge University Press, Cambridge 1995)